PHYSICAL REVIEW A VOLUME 44, NUMBER 9 1 NOVEMBER 1991

# Satellite intensities in the $K$-shell photoionization of CO

J. Schirmer
*Physikalisch-Chemisches Institut, Universität Heidelberg, Im Neuenheimer Feld 253, D-6900 Heidelberg, Germany*

M. Braunstein* and V. McKoy
*Noyes Laboratory of Chemical Physics, California Institute of Technology, Pasadena, California 91125*

(Received 1 April 1991)

A recently proposed scheme for calculating $K$-shell ionization cross sections in atoms and molecules using the relaxed-core Hartree-Fock (RCHF) approximation is extended to the treatment of shakeup processes. As an example, this scheme is applied to the $\pi$-$\pi^*$ satellites in the C 1s photoelectron spectrum of CO. These results for the (S0, $S1$) pair of $\pi$-$\pi^*$ satellite states reveal strong interference effects between the "direct" (bound-free dipole integral) and "conjugate" (bound-free overlap integral) contributions in the transition moment at near-threshold energies. These effects are particularly dominant in the $k\pi$ subchannel and, for the triplet-coupled satellite ($S1$), lead to a drastically increasing cross section with decreasing photon energy. For the singlet-coupled satellite ($S0$) destructive interference leads to a comparatively small cross section near threshold. While these findings may explain the strikingly different behavior of the $S0$ and $S1$ satellite intensities in recent experiments, the present results also show distinct $\sigma$-type shape resonances in both satellite channels at about 10 eV photoelectron energy that are apparently at variance with the experimental evidence. An analysis of the RCHF transition moment via perturbation theory shows that already in first order some potentially important dynmical contributions are missing. In these studies a direct method based on the Schwinger variational principle and single-center expansion techniques is used to obtain the photoelectron orbitals.

PACS number(s): 33.60.Fy, 33.80.Eh

## I. INTRODUCTION

$K$-shell photoelectron spectra of atoms and molecules exhibit, in addition to the $1s$-hole main peak, an intense satellite structure associated with shakeup and shakeoff processes, i.e., valence-electron excitation and ionization, respectively accompanying the $1s$-electron ejection [1,2]. For large photoelectron energies (sudden limit), e.g., realized in Al $K\alpha$ excitation of second-row elements, the relative satellite intensities with respect to the $1s$ main peak are to a good approximation determined by spectroscopic factors reflecting solely bound-state properties of the neutral system and the ion [3,4]. Under such conditions typically 30–40% of the $1s$ cross section is diverted to the shakeup and shakeoff spectrum. Single shake-up peaks with up to 10% of the $1s$-hole main peak intensity have been observed for unsaturated molecules like CO and $N_2$ where excitations to low-lying valence-type $\sigma^*$ and $\pi^*$ orbitals are possible [1,2].

At low photoelectron energies, in particular, near resonances and ionization thresholds, deviations from the "asymptotic" spectral profile can be expected. The dynamical aspects of $K$-shell ionization in atoms and molecules have been the subject of recent experimental studies using tunable synchrotron radiation [5–8]. Surprising intensity variations have been observed at near-threshold energies for the pair of $\pi$-$\pi^*$ satellites in the C $1s$ and N $1s$ photoelectron spectra of CO and $N_2$, respectively [8]. The first satellite, characterized as a $\pi$-$\pi^*$ triplet excitation and having only a small relative intensity in the high-energy limit, becomes drastically enhanced (up to 10% relative to the $1s$ main state) at low photon energies. In contrast, the relative intensity of the second, singlet-coupled, $\pi$-$\pi^*$ satellite decreases steadily from a large value at high photon energy to a rather small value at threshold. The strong enhancement of the first $\pi$-$\pi^*$ satellite in the C $1s$ spectrum of CO was previously inferred by Ungier and Thomas [9] from coincidence measurements combining electron-impact ionization and Auger electron spectroscopy. More recent evidence was found by Medhurst *et al.* [10] studying the C $1s$ ionization of CO by zero-kinetic-energy (ZEKE) spectroscopy.

Previous theoretical studies of photoionization cross sections have been mainly confined to single-hole main states. Among the few examples where satellite intensities have been considered are studies by Ishihara, Mizuno, and Watanabe [11] and by Wijesundra and Kelly [12] on Ne $1s$ and Ar $3s$ satellites, respectively, using methods based on many-body perturbation theory. For molecules we are aware only of a recent study by Årgen and Carravetta [13]. Using a Stieltjes moment theory approach these authors calculate satellite intensities in the O $1s$ shakeup spectrum of water, though only for photon energies in the 1300–1500 eV region. At a less rigorous theoretical level some attempts have been made to understand the near-threshold satellite intensities by means of simple models ("adiabatic limit") based on time-dependent perturbation theory [14–16]. In view of the approximate nature of these models, a more reliable theoretical description based on a proper quantum-mechanical treatment would be highly desirable.

The familiar frozen-core Hartree-Fock (FCHF) approximation, widely used in studies of single-hole ionization [17], cannot be applied to the case of photoelectron

©1991 The American Physical Society

satellites since the corresponding $N$-electron transition moments (photoionization amplitudes) vanish. A more appropriate approach, which maintains the simplicity of the single-particle description, is the relaxed-core Hartree-Fock (RCHF) model. Here, instead of "frozen" ground-state HF orbitals, the "relaxed" orbitals generated by a HF calculation for the ion are used to represent the ionic state and its respective static-exchange potential. Such a description is especially useful in the treatment of $K$-shell ionization since the dominant effect of valence electron relaxation is properly taken into account. In a previous paper [18], henceforth referred to as I, we have discussed in some detail the RCHF approximation and its application to $K$-shell single-hole ionization. In continuation of this study we will here be concerned with RCHF calculations of $K$-shell satellite cross sections. As an exemplary application we shall consider the $\pi$-$\pi^*$ satellites in the C 1$s$ photoelectron spectrum of CO.

The formulation given in I for evaluating the $N$-electron transition amplitude allows one to distinguish between so-called direct and conjugate contributions [19,20]. The latter part arises due to the nonorthogonality between the relaxed continuum orbital and the occupied frozen orbitals and is reflected in the occurrence of bound-free overlap integrals. On the other hand, the direct part, containing the usual bound-free dipole integrals, determines the spectral intensities at large photon energies (sudden limit) since the overlap integrals vanish much more rapidly with photoelectron energy than the dipole integrals. For low photoelectron energies, particularly near ionization thresholds, the conjugate part may, however, become significant. More interestingly, the different selection rules of the conjugate part may allow satellite states to appear near threshold that are forbidden in the high-energy limit due to the monopole selection rules of the direct part. There has been much speculation about the importance of this conjugate shakeup "mechanism" near threshold [5,9,11,19,20]. Here we will give a quantitative study of the direct and conjugate contributions in the near-threshold cross section of molecular photoelectron satellites.

An outline of this paper is as follows. Section II reviews the RCHF formulation of the $K$-shell satellite states and transition amplitudes. In Sec. III an analysis of the RCHF description is given via a comparison with the exact amplitude through first-order perturbation theory. Details of the calculations are given in Sec. IV, while Sec. V contains the discussion of our results. A summary of our findings and some conclusions are given in Sec. VI.

## II. THEORY

### A. Transition moments for K-shell photoelectron satellites in the relaxed-core Hartree-Fock approximation

In the following we will briefly review the essential features of the relaxed-core Hartree-Fock (RCHF) approximation and then discuss its specific application to the case of core-hole satellite states. A more detailed discussion of this approach has been given in our previous article I. The basic assumption in a single-particle description of photoionization such as the frozen- and relaxed-core HF model, is the representation of the $N$-electron final state as the (antisymmetrized) product of the ionic state $|\Psi_n^{N-1}\rangle$ and the photoelectron continuum orbital $|\psi_k^{(-)}\rangle$ (with incoming-wave boundary condition). Using the second-quantized notation $c_k^\dagger$ for the creation operator associated with the continuum orbital $|\psi_k^{(-)}\rangle$ we may write

$$|\Psi_{n,k}^N\rangle = c_k^\dagger |\Psi_n^{N-1}\rangle \; . \tag{1}$$

The normalization properties of the continuum orbitals can be transferred to the $N$-electron final states provided that the orthogonality constraints

$$c_k |\Psi_n^{N-1}\rangle = 0 \tag{2}$$

are fulfilled.

Using the product approximation (1) for the final state, the $N$-electron transition amplitudes

$$A_{n,k}^{(\mu)} = \langle \Psi_{n,k}^N | \hat{D}^{(\mu)} | \Psi_0^N \rangle \tag{3}$$

can be written in the more explicit form [20–22]

$$A_{n,k}^{(\mu)} = \sum_r \langle \psi_k^{(-)} | \hat{d}^{(\mu)} | \phi_r \rangle x_r^{(n)} + \sum_r \langle \psi_k^{(-)} | \phi_r \rangle y_r^{(n)} \; , \tag{4a}$$

where

$$x_r^{(n)} = \langle \Psi_n^{N-1} | a_r | \Psi_0^N \rangle \tag{4b}$$

and

$$y_r^{(n)} = \langle \Psi_n^{N-1} | \hat{D} a_r | \Psi_0^N \rangle \; . \tag{4c}$$

In Eqs. (3) and (4), $|\Psi_0^N\rangle$ denotes the initial $N$-electron ground state, and

$$\hat{D}^{(\mu)} = \sum_{i=1}^{N} \hat{d}_i^{(\mu)} \tag{5}$$

is an $N$-electron transition operator, e.g., the $\mu$th component of the dipole operator. In Eq. (4) a representation in terms of "frozen" ground state HF orbitals $|\phi_r\rangle$ and the associated second-quantized operators $a_r(a_r^\dagger)$ is assumed. According to Eq. (4) we may distinguish two contributions to the transition amplitude. The first sum on the right-hand side of Eq. (4), referred to as the direct part ($A^{\text{I}}$), combines the bound-free dipole integrals $\langle \psi_k^{(-)} | \hat{d} | \phi_r \rangle$ and the $(N-1)$-particle overlap or spectroscopic amplitudes $x_r^n$. The second sum ($A^{\text{II}}$) contains products of the bound-free overlap integrals $\langle \psi_k^{(-)} | \phi_r \rangle$ and the $(N-1)$-particle transition moments $y_r^{(n)}$. This contribution, arising from the nonorthogonality of the continuum and the (frozen) HF orbitals, is called the conjugate part [19,20]. For large photoelectron energies the overlap integrals $\langle \psi_k^{(-)} | \phi_r \rangle$ vanish much more rapidly than the dipole integrals $\langle \psi_k^{(-)} | \hat{d} | \phi_r \rangle$. Thus, in the limit of high photon energy (sudden limit) the photoelectron intensities are solely determined by the direct part [3]. Near photoionization thresholds, however, the conjugate part may play an important role. In particular, different selection rules for the conjugate part may allow ionic states forbidden by the selection rules of the direct part.

In addition to the product approximation (1) the following three approximations are introduced in the RCHF model.

(i) The ground-state HF representation

$$|\Phi_0^N\rangle = |\phi_1\phi_2 \cdots \phi_N| \tag{6}$$

is used for the initial state $|\Psi_0^N\rangle$.

(ii) The ionic state is represented in terms of "relaxed" orbitals generated by a HF calculation for the ion. Let $|\psi_r\rangle$ denote the relaxed orbitals and $c_r^\dagger(c_r)$ the associated creation (removal) operators of second quantization. Then, an ionic single-hole state may be written as

$$|\Psi_h^{N-1}\rangle = c_h|\overline{\Phi}_0^N\rangle \tag{7}$$

where the "relaxed" $N$-particle state

$$|\overline{\Phi}_0^N\rangle = |\psi_1\psi_2 \cdots \psi_N| \tag{8}$$

is defined analogously to $|\Phi_0^N\rangle$ of Eq. (6) as the Slater determinant of the lowest relaxed orbitals $|\psi_r\rangle$. Similarly, we may represent a two-hole–one-particle $(2h-1p)$ satellite state describing a hole in the occupied orbitals $h$ and $l$ $(n_h = n_l = 1)$ and an electron in the unoccupied orbital $j$ $(\overline{n}_j = 1 - n_j = 1)$ by

$$|\Psi_{jhl}^{N-1}\rangle = c_j^\dagger c_h c_l|\overline{\Phi}_0^N\rangle \ . \tag{9}$$

The construction of symmetry adapted satellite states is addressed in Sec. II B.

(iii) The scattering orbitals $|\psi_k^{(-)}\rangle$ are determined by solving the single-particle scattering equation using the static-exchange (HF) potential of the relaxed ion under appropriate boundary, normalization, and orthogonality conditions. Explicit RCHF satellite potentials will be given in Sec. II C.

As discussed in I, complications arise in the RCHF approximation due to nonorthogonality between the frozen and the relaxed orbitals used in representing the initial and final $N$-electron state, respectively. In the case of $K$-shell ionization, however, these problems can be eliminated in a well-defined manner, namely by using the core-valence separation (CVS) approximation which can be justified by the large energy gap between core and valence levels and the small coupling integrals for states with different core orbital occupations. Within this approximation the relaxed and frozen $1s$ orbital, henceforth denoted by $|\psi_c\rangle$ and $|\phi_c\rangle$, respectively, become identical and the following orthogonality relations hold:

$$\langle\psi_r|\phi_c\rangle = 0 \ , \quad r \neq c \ , \tag{10}$$

$$\langle\psi_k^{(-)}|\phi_c\rangle = 0 \ . \tag{11}$$

Using these relations the general expressions derived in I for the RCHF transition moments simplify considerably. Moreover, all artificial contributions to the RCHF amplitude arising from the lack of strict orthogonality of the initial and final $N$-electron states vanish. The final result for the $K$-shell satellite transition amplitude in the RCHF and CVS approximations can be written as

$$\begin{aligned} A_{jcl,k} = (&-\langle\langle\psi_k^{(-)}|\hat{d}|\phi_c\rangle\rangle\langle\langle\psi_j|\phi_l\rangle\rangle \\ &+\langle\langle\psi_j|\hat{d}|\phi_c\rangle\rangle\langle\langle\psi_k^{(-)}|\phi_l\rangle\rangle)\langle\overline{\Phi}_0^N|\Phi_0^N\rangle \ . \end{aligned} \tag{12a}$$

This result has the form of the simplified expressions given previously for shakeup amplitudes [19,20]. In Eq. (12a), however, the simple overlap and dipole integrals have to be replaced by effective quantities defined as follows:

$$\langle\langle\psi_i|\phi_l\rangle\rangle = \sum_r \langle\psi_i|\phi_r\rangle(\underline{S}^{-1})_{rl} \ , \tag{12b}$$

$$\begin{aligned} \langle\langle\psi_i|\hat{d}|\phi_c\rangle\rangle = &\langle\psi_i|\hat{d}|\phi_c\rangle \\ &- \sum_{r,r'} \langle\psi_i|\phi_r\rangle(\underline{S}^{-1})_{r,r'}\langle\psi_{r'}|\hat{d}|\phi_c\rangle \ . \end{aligned} \tag{12c}$$

Here $\underline{S}$ denotes the matrix of relaxed-frozen overlap integrals

$$S_{pq} = \langle\psi_p|\phi_q\rangle \tag{13}$$

for occupied orbitals $(n_p = n_q = 1)$; the summations in Eqs. (12b) and (12c) run over occupied orbitals only. The overlap matrix element $\langle\overline{\Phi}_0^N|\Phi_0^N\rangle$ of the frozen and relaxed Slater determinants in Eq. (12a) is given by the determinant of $\underline{S}$:

$$\langle\overline{\Phi}_0^N|\Phi_0^N\rangle = \det(\underline{S}) \ . \tag{14}$$

By comparing Eqs. (12a)–(12c) with the form given for the transition amplitude in Eqs. (4a) and (4b) we can easily specify the bound-state amplitudes $x_r^{(jcl)}$ and $y_r^{(jcl)}$ in the RCHF approximation. The result for the spectroscopic amplitude $x_r^{(jcl)}$ is

$$x_r^{(jcl)} = -\delta_{rc}\langle\langle\psi_j|\phi_l\rangle\rangle\langle\overline{\Phi}_0^N|\Phi_0^N\rangle \ . \tag{15}$$

Thus, the direct part of the transition moment may be written as

$$A_{jcl,k}^{\mathrm{I}} = \langle\psi_k^{(-)}|\hat{d}|\phi_c\rangle x_c^{(jcl)} \ . \tag{16}$$

Comparison of the direct part of the full amplitude of Eq. (12) shows more clearly the effect of the conjugate contributions. First, the dipole integral in the direct part (Eq. 16) is modified essentially by removing the occupied frozen orbital admixtures in $|\psi_k^{(-)}\rangle$. This leads to an "effective" direct part [first contribution on the right-hand side of Eq. (12a)]. Second, this part is augmented by another contribution referred to as the effective conjugate shakeup part in which the role of the orbitals $k$ and $j$ is exchanged. According to the usual interpretation the (effective) direct amplitude corresponds to a "direct process" in which a bound-free (dipole) transition $c \rightarrow k$ is accompanied by a bound-bound (monopole shakeup $l \rightarrow j$; the (effective) conjugate shakeup amplitude, on the other hand, arises due to a "conjugate shakeup process," i.e., the bound-bound dipole transition $c \rightarrow j$ plus the bound-free monopole shakeup (off) $l \rightarrow k$. The transition amplitude $A_{jcl,k}$ of Eq. (12a) may be complemented by the contribution

$$A'_{jcl,k}=(\langle\!\langle \psi_k^{(-)}|\hat{d}|\phi_l\rangle\!\rangle\langle\!\langle\psi_j|\phi_c\rangle\!\rangle - \langle\!\langle\psi_j|\hat{d}|\phi_l\rangle\!\rangle\langle\!\langle\psi_k^{(-)}|\phi_c\rangle\!\rangle)\langle\bar{\Phi}_0^N|\Phi_0^N\rangle\ ,$$

which is formally obtained from $-A_{jcl,k}$ by exchanging $c$ and $l$. Obviously these additional direct and conjugate amplitudes do not play a role for *K*-shell satellites since the effective overlaps $\langle\!\langle\psi_j|\phi_c\rangle\!\rangle$ and $\langle\!\langle\psi_k^{(-)}|\phi_c\rangle\!\rangle$ vanish in the CVS approximation.

The expressions given above for the satellite amplitudes correspond to "primitive" product states $c_k^\dagger c_j^\dagger c_c c_l|\Phi_0^N\rangle$ where $k$, $j$, $c$, and $l$ denote spin orbitals. Spin-free expressions applying to final states of proper spin and spatial symmetry are easily obtained by appropriate linear combinations of the primitive amplitudes and by evaluating the spin degrees of freedom. In the ensuing Secs. II B and II C we shall briefly discuss the choice of the symmetry adapted satellite states and their static-exchange potentials. Examples of spin-free expressions for the satellite cross sections are given in Sec. V.

### B. *K*-shell hole satellite states

Symmetry-adapted ionic states can straightforwardly be constructed in the FCHF or RCHF approximation as linear combinations of primitive states. The case of $2h$-$1p$ satellites, however, requires some comment since here two independent doublet states can be formed, the choice of which is not unique. For simplicity, let us consider the case of the satellite configuration $(j^1c^{-1}l^{-1})$ with spatially nondegenerate orbitals $j$, $c$, and $l$. For the moment we shall split the general one-particle quantum numbers $j$ into a spatial quantum number $j$ and a (magnetic) spin quantum number $\gamma=\alpha,\beta(=\pm\frac{1}{2})$. The eight primitive spin states

$$(\gamma\kappa\lambda)\equiv|\Psi^{N-1}_{j\gamma c\kappa l\lambda}\rangle$$

associated with the specific spatial configuration can be combined to form a set of quartet states $(S=\frac{3}{2})$ and two independent sets of doublet states $(S=\frac{1}{2})$. One way to choose the two doublet states $(M=-\frac{1}{2})$ is as follows:

$$|{}^2\Psi_{jcl}(0)\rangle=\frac{1}{\sqrt{2}}[(\beta\alpha\beta)+(\alpha\alpha\alpha)]\ , \tag{17a}$$

$$|{}^2\Psi_{jcl}(1)\rangle=\frac{1}{\sqrt{6}}[-(\beta\alpha\beta)+2(\beta\beta\alpha)+(\alpha\alpha\alpha)]\ . \tag{17b}$$

Note that a particle-hole notation [see Eq. (9)] is assumed here. This corresponds to a coupling scheme in which the valence electrons in orbital $j$ and $l$ form an intermediate singlet $(S'=0)$ and triplet $(S'=1)$, respectively. In general, this particular coupling scheme is not distinguished from other possibilities. However, for the case of *K*-shell satellites with $j$ being a valence-type ($\pi^*$ or $\sigma^*$) orbital, the states according to Eq. (17) are an optimal zeroth-order representation of the actual eigenstates of the Hamiltonian. As discussed in Ref. [23] the coupling matrix element for the two doublet states (17) contains only core-valence exchange integrals and its absolute value is hence small; the (first-order) energy separation, on the other hand, is essentially given by twice the valence exchange integral $K_{jl}$ which can assume considerably larger values.

Doublet satellite states with intermediate spin $S'=0$ and 1, respectively, can likewise be constructed if the orbitals involved are spatially degenerate, e.g., for the $\pi$-$\pi^*$ *K*-shell satellites in CO considered below. The latter satellite configuration gives rise to two (monopole-allowed) doublet states ${}^2\Sigma^+(S')$ and moreover similar pairs of ${}^2\Sigma^-$ and ${}^2\Delta$ states. In Table I we have specified for these states (choosing $M_s=\frac{1}{2}$) the normalization constants and the expansion coefficients with respect to the primitive states, where, e.g., $[\pi_x^*\beta, 1s\alpha, \pi_x\beta]$ is a shorthand notation for the state $|\phi^{N-1}_{\pi_x^*\beta, 1s\alpha, \pi_x\beta}\rangle$ as defined by Eq. (9).

TABLE I. Normalization constants and expansion coefficients for the symmetry-adapted RCHF states corresponding to the satellite configuration $(\pi^*)^1(1s)^{-1}(\pi)^{-1}$.

| | ${}^2\Sigma^+(0)$ | ${}^2\Sigma^+(1)$ | ${}^2\Sigma^-(0)$ | ${}^2\Sigma^-(1)$ | ${}^2\Delta_x(0)$ | ${}^2\Delta_x(1)$ |
|---|---|---|---|---|---|---|
| Normalization coefficients | | | | | | |
| | 1/2 | $1/\sqrt{12}$ | 1/2 | $1/\sqrt{12}$ | 1/2 | $1/\sqrt{12}$ |
| Expansion coefficients | | | | | | |
| $[\pi_x^*\beta, 1s\alpha, \pi_x\beta]$ | 1 | −1 | | | 1 | −1 |
| $[\pi_x^*\beta, 1s\beta, \pi_x\alpha]$ | 0 | 2 | | | 0 | 2 |
| $[\pi_x^*\alpha, 1s\alpha, \pi_x\alpha]$ | 1 | 1 | | | 1 | 1 |
| $[\pi_y^*\beta, 1s\alpha, \pi_y\beta]$ | 1 | −1 | | | −1 | 1 |
| $[\pi_y^*\beta, 1s\beta, \pi_y\alpha]$ | 0 | 2 | | | 0 | −2 |
| $[\pi_y^*\alpha, 1s\alpha, \pi_y\alpha]$ | 1 | 1 | | | −1 | −1 |
| $[\pi_x^*\beta, 1s\alpha, \pi_y\beta]$ | | | 1 | −1 | | |
| $[\pi_x^*\beta, 1s\beta, \pi_y\alpha]$ | | | 0 | 2 | | |
| $[\pi_x^*\alpha, 1s\alpha, \pi_y\alpha]$ | | | 1 | 1 | | |
| $[\pi_y^*\beta, 1s\alpha, \pi_x\beta]$ | | | −1 | 1 | | |
| $[\pi_y^*\beta, 1s\beta, \pi_x\alpha]$ | | | 0 | −2 | | |
| $[\pi_y^*\alpha, 1s\alpha, \pi_x\alpha]$ | | | −1 | −1 | | |

### C. Static-exchange potentials for satellite states

Similar to the case of single-hole main states (see the discussion in I) one may derive single-particle scattering equations of the form

$$(\hat{t}+\hat{v}-\tfrac{1}{2}k^2)|\psi_k^{(-)}\rangle=0 \tag{18}$$

for the continuum in the static-exchange field associated with the ionic $2h-1p$ satellite state. In Eq. (18) the operator $\hat{t}$ contains the kinetic energy and the Coulomb interaction with the nuclei, while $\hat{v}$ is associated with the electron-electron interaction. To obtain the appropriate potential the variational principle [24]

$$\langle \delta\Psi_{jcl,k}^{N}|\hat{H}-E|\Psi_{jcl,k}^{N}\rangle=0 \tag{19}$$

is applied to the $N$-electron final state

$$|\Psi_{jcl,k}^{N}\rangle=c_k^{\dagger}c_j^{\dagger}c_c c_l|\overline{\Phi}_0^{N}\rangle \tag{20}$$

constructed from the fixed "target" state $|\Psi_{jcl}^{N-1}\rangle$ and the continuum orbital $|\psi_k^{(-)}\rangle$. Only the continuum orbital is varied in $|\delta\Psi_{jcl,k}^{N}\rangle$. The variational principle yields Eq. (18) readily if orthogonality is assumed between the (spatial) continuum orbital $|\psi_k^{(-)}\rangle$ and both the doubly and singly occupied (spatial) orbitals in $|\Psi_{jcl}^{N-1}\rangle$. Without this orthogonality constraint the equations are much more complicated. For the two doublet states specified in Eqs. (17a) and (17b), respectively, and assuming a final $N$-electron singlet state the potentials $\hat{v}(S')$ become [23], for singlet states,

$$\hat{v}(0)=\sum_{i\neq c,l}(2\hat{J}_i-\hat{K}_i)n_i+\hat{J}_c+\hat{K}_c+\hat{J}_l-\tfrac{1}{2}\hat{K}_l+\hat{J}_j-\tfrac{1}{2}\hat{K}_j\ , \tag{21a}$$

and for triplet states,

$$\hat{v}(1)=\hat{v}(0)-2\hat{K}_c+\hat{K}_l+\hat{K}_j\ . \tag{21b}$$

Here $\hat{J}_i$ and $\hat{K}_i$ denote Coulomb and exchange operators, respectively, associated with the relaxed orbitals $|\psi_i\rangle$. The two potentials differ only with respect to the sign of the exchange operators for the open-shell orbitals $j$, $c$, and $l$. The orthogonality properties imposed on the continuum orbitals do not follow automatically from solving Eq. (18) but have to be imposed as additional constraints. The potentials used for the ${}^2\Sigma^+(S')$ states of the $\pi$-$\pi^*$ satellite manifold (as specified in Sec. II B) are

$$\hat{v}({}^2\Sigma^+(0))=\sum_{i\neq 1s,\pi_x,\pi_y}(2\hat{J}_i-\hat{K}_i)+\hat{J}_{1s}+\hat{K}_{1s}+3\hat{J}_{\pi}-\tfrac{3}{2}\hat{K}_{\pi}+\hat{J}_{\pi^*}-\tfrac{1}{2}\hat{K}_{\pi^*} \tag{21c}$$

and

$$\hat{v}({}^2\Sigma^+(1))=\hat{v}({}^2\Sigma^+(0))-2\hat{K}_{1s}+\hat{K}_{\pi}+\hat{K}_{\pi^*}\ , \tag{21d}$$

where $\hat{J}_{\pi}=\frac{1}{2}(\hat{J}_{\pi_x}+\hat{J}_{\pi_y})$ and $\hat{K}_{\pi}=\frac{1}{2}(\hat{K}_{\pi_x}+\hat{K}_{\pi_y})$.

## III. ANALYSIS OF THE RCHF SATELLITE CROSS SECTION

The potential and limitations of the RCHF approximation can be seen more clearly by comparing the exact transition amplitude with the RCHF result through first order of perturbation theory. Such an analysis has been presented in I for the single-hole main states. Here we discuss the case of $2h$-$1p$ $K$-shell satellite states.

In zeroth order, i.e., in the FCHF representation, the corresponding $N$-electron final state is given by

$$|\Phi_{kjcl}^{N}\rangle=a_k^{\dagger}a_j^{\dagger}a_c a_l|\Phi_0^{N}\rangle\ . \tag{22}$$

Here $a_k^{\dagger}$ is associated with the HF continuum orbital $|\phi_k^{(-)}\rangle$; for simplicity, we restrict ourselves to primitive states, i.e., $k$, $j$, $c$, and $l$ denote spin orbitals. Obviously the transition amplitude vanishes in zeroth order:

$$A_{jcl,k}^{(0)}=\langle \Phi_{kjcl}^{N}|\hat{D}|\Phi_0^{N}\rangle=0\ . \tag{23}$$

The first-order contributions are

$$A_{jcl,k}^{(1)}=\langle \Psi_{kjcl}^{(1)}|\hat{D}|\Phi_0^{N}\rangle+\langle \Phi_{kjcl}^{N}|\hat{D}|\Psi_0^{(1)}\rangle\ . \tag{24}$$

Here $|\Psi_{kjcl}^{(1)}\rangle$ and $|\Psi_0^{(1)}\rangle$ denote the first-order final and initial states, respectively. For $|\Psi_{kjcl}^{(1)}\rangle$ in the first term on the right-hand side of Eq. (24) the $np$-$nh$ excitations with $n\geq 2$ do not contribute; accordingly we obtain

$$A_{jcl,k}^{(1)}=\langle p\text{-}h|\hat{D}|\Phi_0^{N}\rangle-\frac{V_{kj|cl|}}{\varepsilon_k+\varepsilon_j-\varepsilon_c-\varepsilon_l}\langle \Phi_0^{N}|\hat{D}|\Phi_0^{N}\rangle+\langle \Phi_{kjcl}^{N}|\hat{D}|\Psi_0^{(1)}\rangle\ . \tag{25}$$

Here the first term is explicitly given by

$$\begin{aligned}\langle p\text{-}h|\hat{D}|\Phi_0^{N}\rangle={}&\sum_{c'}\langle k|\hat{d}|c\rangle\frac{V_{c'j[cl]}-\delta_{cc'}V_{kj[kl]}}{\varepsilon_j-\varepsilon_l}\\&+\sum_{c'}\langle j|\hat{d}|c'\rangle\frac{-V_{c'k[cl]}+\delta_{cc'}V_{kj[lj]}}{\varepsilon_k-\varepsilon_l}\\&-\sum_{k'\neq j,k}\langle k'|\hat{d}|c\rangle\frac{V_{kj[k'l]}}{\varepsilon_k+\varepsilon_j-\varepsilon_l-\varepsilon_{k'}}\ .\end{aligned} \tag{26}$$

For simplicity, the CVS approximation has been used here; $c'$ is allowed to differ from $c$ only in the spin quantum number. The three terms on the right-hand side of Eq. (26) arise from the admixture of the single excitations $(k^1c^{-1})$, $(j^1c^{-1})$, and $(k'^1c^{-1})$ in the final $N$-electron state.

The second term in Eq. (25) can be combined with the third term arising from ground-state correlation. The resulting part is denoted $A_{jcl,k}^{C}(1)$ and is

$$\begin{aligned}A_{jcl,k}^{C}(1)={}&\sum_{r}\gamma_{rjcl}\langle k|\hat{d}|r\rangle\bar{n}_r+\sum_{s}\gamma_{kscl}\langle j|\hat{d}|s\rangle\bar{n}_s\\&-\sum_{v}\gamma_{kjcv}\langle v|\hat{d}|l\rangle n_v-\sum_{u}\gamma_{kjul}\langle u|\hat{d}|c\rangle n_u\ .\end{aligned} \tag{27}$$

Here the abbreviation

$$\gamma_{rsuv}=\frac{V_{rs[uv]}}{\varepsilon_r+\varepsilon_s-\varepsilon_u-\varepsilon_v} \tag{28}$$

is used; the summations are restricted by the HF occupation numbers ($n_i=1-\bar{n}_i=1,0$). In the CVS approximation only the last term in Eq. (27) survives, and the ground-state correlation contribution in the first-order amplitude becomes

$$A^{C}_{jcl,k}(1)=\sum_u \frac{V_{kj[lu]}}{\varepsilon_k+\varepsilon_j-\varepsilon_l-\varepsilon_u}\langle u|\hat{d}|c\rangle n_u \ . \tag{29}$$

Obviously this contribution arises from admixtures of double excitations ($k^1j^1l^{-1}u^{-1}$) in the ground state $|\Psi_0^N\rangle$.

The perturbation expansion of the RCHF amplitude [Eqs. (14)–(16),(20)] is easily obtained. Again, there is no zeroth-order contribution,

$$A^{RC}_{jcl,k}(0)=0 \tag{30}$$

since the zeroth-order overlaps $\langle\phi_k^{(-)}|\phi_l\rangle$ and $\langle\phi_j|\phi_l\rangle$ vanish. In first-order the RCHF and CVS approximations lead to the following result:

$$A^{RC}_{jcl,k}(1)=-\langle k|\hat{d}|c\rangle\langle\psi_j^{(1)}|l\rangle+\langle j|\hat{d}|c\rangle\langle\psi_k^{(1)}|l\rangle \tag{31a}$$

where

$$\langle\psi_j^{(1)}|l\rangle=(\varepsilon_j-\varepsilon_l)^{-1}(-V_{jclc}+\gamma_1 V_{jccl}) \tag{31b}$$

and

$$\langle\psi_k^{(1)}|l\rangle=(\varepsilon_k-\varepsilon_l)^{-1}(-V_{kclc}+\gamma_2 V_{kccl} +V_{kjlj}+\gamma_3 V_{kjjl}) \ . \tag{31c}$$

The coefficients $\gamma_1$, $\gamma_2$, and $\gamma_3$ of the exchange integrals in Eq. (31) depend on the details of the methods used to determine the relaxed bound and continuum orbitals and are not of interest here. In deriving the expressions Eqs. (31a) and (31b) the RCHF potentials Eq. (21) and the orthogonality conditions $\langle\psi_j|\psi_l\rangle=0$ and $\langle\psi_k^{(-)}|\psi_l\rangle=0$ have been assumed.

Comparison of the exact and the RCHF amplitude shows discrepancies already in first order of perturbation theory. Apart from the "nondiagonal" third term in Eq. (26) and exchange integrals, there is a "polarization" contribution

$$A^{P}_{jcl,k}(1)=-\langle k|\hat{d}|c\rangle\frac{V_{kj[kl]}}{\varepsilon_j-\varepsilon_l} \tag{32}$$

in the exact amplitude that has no counterpart in the RCHF result. The quantity

$$-(\varepsilon_j-\varepsilon_l)^{-1}V_{kj[kl]}$$

can be viewed as a nonorthogonality contribution to $\langle\phi_j^{(1)}|\phi_l\rangle$ induced by the continuum electron in the state $k$. In the RCHF model, of course, such a polarization effect is not accounted for. Another shortcoming of the RCHF approximation is the neglect of the ground-state correlation contribution $A^{C}_{jcl,k}(1)$ given by Eq. (29). Both the polarization and correlation contributions depend strongly on the photoelectron energy and may play an essential role near threshold. This means that the conjugate shakeup amplitude included in the RCHF model is not the only dynamically important part of the full satellite transition amplitude. The neglect of the other two dynamical first-order contributions may seriously affect the quality of the RCHF description.

## IV. CALCULATIONS

The RCHF model described above was applied to the pair of $(2\pi)^1(2\sigma)^{-1}(1\pi)^{-1}(^2\Sigma^+)$ satellites in the C 1*s* photoelectron spectrum of CO. The computational procedures were essentially the same as in our previous calculations of the 1*s* single-hole ionization and we refer the reader to the description given in I for more details. Hartree-Fock (HF) calculations of good quality (as defined in I) were performed for the neutral CO molecule and the C 1*s* single-hole state of CO$^+$. The relaxed orbitals generated by the latter HF calculation were chosen to represent both the $\pi$-$\pi^*$ triplet ($S1$) and singlet ($S0$) satellite state, respectively, with the first virtual (unoccupied) $\pi$ orbital used as the $\pi^*$ orbital. The explicit expressions for the satellite wave functions and the associated static-exchange potentials are as specified by Table I and Eqs. (21), respectively.

The one-electron Schrödinger equation for the photoelectron orbitals was solved using an iterative method based on the Schwinger variational principle and single-center expansion technique [25,26]. Details of these calculations are discussed in I. Single-center expansions and numerical radial integrations were also used to calculate the overlap and dipole integrals for bound and continuum orbitals. The size of the various expansions and the grid parameters for the numerical integrations have been given in I.

The total photoionization cross section averaged over molecular orientations is given by the expression (in atomic units)

$$\sigma=\frac{4\pi^2}{3c}\omega k\sum_{lm\mu}|I_{lm\mu}|^2 \ . \tag{33}$$

Here $\omega$ is the photon energy, $k$ is the magnitude of the photoelectron momentum, and $I_{lm\mu}$ denote spin-free transition amplitudes defined with respect to the partial waves $\psi_{klm}^{(-)}(\mathbf{r})$ in the partial-wave expansion

$$\psi_k^{(-)}(\mathbf{r})=\left[\frac{2}{\pi}\right]^{1/2}\sum_{lm}\frac{i^l}{k}\psi_{klm}^{(-)}(\mathbf{r})Y_{lm}^*(\hat{\mathbf{k}}) \tag{34}$$

of the continuum orbital. The asymmetry parameter $\beta$ of the photoelectron angular distribution is calculated according to Eq. (94) of I. For the singlet-coupled satellite $S0$ the amplitude $I_{lm\mu}$ is given by

$$I_{lm\mu}(0)=\sqrt{2}[x_{1s}(0)\langle\langle\psi_{klm}^{(-)}|\hat{r}_\mu|\phi_{1s}\rangle\rangle +\tfrac{1}{2}\langle\bar{\Phi}_0^N|\Phi_0^N\rangle\langle\langle\psi_{\pi^*\bar{\mu}}|\hat{r}_\mu|\phi_{1s}\rangle\rangle\langle\langle\psi_{klm}^{(-)}|\phi_{\pi\bar{\mu}}\rangle\rangle]. \tag{35a}$$

Here the dipole operator components refer to the spherical components

$$\hat{r}_\mu = \begin{cases} \mp(\hat{x} \pm i\hat{y})\sqrt{2} & \text{for } \mu = \pm 1 , \\ \hat{z} & \text{for } \mu = 0 , \end{cases}$$

and $\bar{\mu} = \pm$ for $\mu = \pm 1$. The effective overlap and dipole integrals are defined as in Eqs. (12b) and (12c), respectively, with spin-free orbitals used throughout. Since CO has only one occupied $\pi$ orbital some of these quantities simplify considerably, e.g.,

$$\langle\langle \psi_{klm}^{(-)} | \phi_{\pi_\pm} \rangle\rangle = \langle \psi_{klm}^{(-)} | \phi_{\pi_\pm} \rangle \langle \psi_{\pi_\pm} | \phi_{\pi_\pm} \rangle^{-1} ,$$

$$\begin{aligned} \langle\langle \psi_{\pi_+^*} | \hat{r}_1 | \phi_{1s} \rangle\rangle = {} & \langle \psi_{\pi_+^*} | \hat{r}_1 | \phi_{1s} \rangle \\ & - \langle \psi_{\pi_+^*} | \phi_{\pi_+} \rangle \langle \psi_{\pi_+} | \phi_{\pi_+} \rangle^{-1} \\ & \times \langle \psi_{\pi_+} | \hat{r}_1 | \phi_{1s} \rangle . \end{aligned}$$

In Eq. (35a), $x_{1s}(0)$ denotes the spin-free spectroscopic amplitude [Eq. (15)] in the RCHF approximation,

$$x_{1s}(0) = -2 \langle \bar{\Phi}_0^N | \Phi_0^N \rangle \langle\langle \psi_{\pi_+} | \phi_{\pi_+} \rangle\rangle . \tag{35b}$$

Similarly to Eq. (35a), the spin-free amplitude $I_{lm\mu}(1)$ for the triplet-coupled satellite $S1$ is

$$\begin{aligned} I_{lm\mu}(1) = \sqrt{2} [ & x_{1s}(1) \langle\langle \psi_{klm}^{(-)} | \hat{r}_\mu | \phi_{1s} \rangle\rangle \\ & + (\sqrt{3}/2) \langle \bar{\Phi}_0^N | \Phi_0^N \rangle \langle\langle \psi_{\pi^* \bar{\mu}} | \hat{r}_\mu | \phi_{1s} \rangle\rangle \\ & \times \langle\langle \psi_{klm}^{(-)} | \phi_{\pi\bar{\mu}} \rangle\rangle ] . \end{aligned} \tag{36}$$

In the strict RCHF model the spectroscopic amplitude $x_{1s}(1)$ for $S1$ vanishes and the (effective) direct part does not contribute at all. Obviously, this is an oversimplification and disagrees with the experimental relative intensity of $S1$ in the high-energy limit. Deviating from the RCHF prescription we here use the more realistic value of $x_{1s} = 0.123$ obtained from a recent Green's function study [27]. For consistency we have also replaced the RCHF result of $x_{1s}(0) = -0.227$ for $S0$ by the corresponding Green's function value $-0.185$. This choice reduces the $S0$ cross section by about 40% at high photon energy and leads to good agreement between the theoretical and observed relative satellite intensities in the high-energy limit.

The numerical values of the relaxed-frozen overlap and dipole integrals for the occupied orbitals have been listed in Table I in I. The additional integrals required here are $\langle \psi_\pi^* | \phi_\pi \rangle = 0.1256$ and $\langle \psi_\pi^* | r_1 | \phi_{1s} \rangle = -0.0581$ a.u. (where $1s = 2\sigma$ and $\pi^* = 2\pi$).

## V. RESULTS AND DISCUSSION

The first two shakeup satellites in the C 1s photoelectron spectrum of CO are found 8.3 and 14.9 eV, respectively, above the single-hole main line at 296.2 eV binding energy [1,28]. The assignment of these peaks to a triplet ($S1$) and singlet ($S0$)$\pi$-$\pi^*$ excitation in addition to the C 1s hole has been confirmed by Guest *et al.* [29] on the basis of large-scale configuration-interaction (CI) calculations. The satellite intensities in the high-energy (Al $K\alpha$) spectrum [1,28] are 2.3% for $S1$ and 4.8% for $S0$ relative to the C 1s main peak. Theoretical intensity ratios (2.2% for $S1$ and 5.0% for $S0$) in very good agreement with the experimental values were obtained by Angonoa, Walter, and Schirmer [27] using Green's function (GF) methods. Both the CI and the GF studies show that the higher lying satellite state $S0$ has already substantial admixtures of $\pi$-$\pi^*$ double excitations.

Figure 1 shows the calculated $S1$ and $S0$ satellite cross sections from the respective experimental thresholds (304.5 and 311.1 eV) up to 400 eV photon energy. Both curves exhibit broad shape-resonance structures centered 10–11 eV above threshold. While for the triplet satellite $S1$ the resonance peak appears to be growing out of a distinctly rising (towards threshold) background, the resonance in the $S0$ channel is superimposed on the declining wing of a broad structure with a maximum at 350 eV. At threshold the $S1$ cross section is about there times larger than that for $S0$. The two curves cross each other between the $S1$ and $S0$ resonance positions. Without the resonance enhancements the crossing point would be considerably higher, namely around 330 eV. Above this point the satellite intensities approach the theoretical high-energy ratio of 2.2/5.0.

Figures 2 and 3 show for $S0$ and $S1$, respectively, the decomposition of the cross section into the separate contributions of the $k\sigma$ and $k\pi$ subchannels. Also plotted (broken line) are the "direct" cross sections obtained by omitting the conjugate contributions in the amplitudes (35) and (36). We see that the resonant behavior is specific to the $k\sigma$ channel, while the $k\pi$ cross sections are nonresonant. Similar to the case of C 1s single-hole ionization, we may identify the resonances in the satellite channels as $\sigma^*$ shape resonances, here associated with quasibound double excitations of the type $(1s)^{-1}(1\pi)^{-1}(2\pi)^1(\sigma^*)^1$, where $\sigma^*$ is the unoccupied valence-type $\sigma$ orbital derived from the $2p$ atomic orbitals. Distinct differences can be observed with respect to the height, width, and shape of the resonances for $S0$ and $S1$. The effect of the conjugate contributions in the $k\sigma$

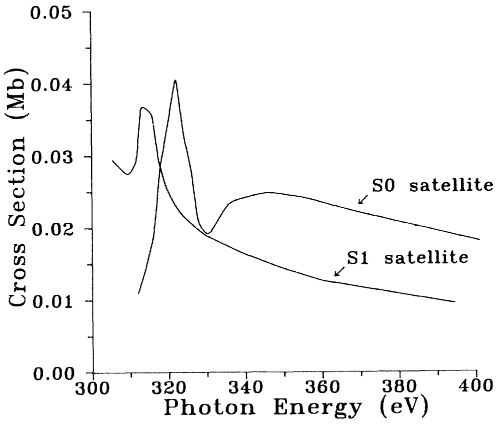

FIG. 1. Calculated photoionization cross sections (RCHF approximation and length form) for the $^2\Sigma^+(\pi$-$\pi^*)$ satellites ($S1$ and $S0$) of CO$^+$ (C $1s^{-1}$).

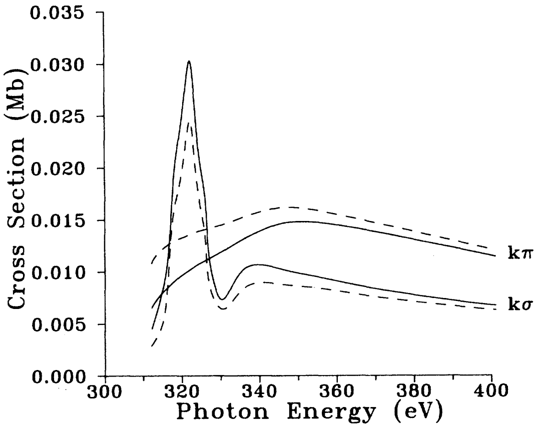

FIG. 2. Partial channel photoionization cross sections for the $S0$ satellite of $CO^+$ (C $1s^{-1}$): ——, direct plus conjugate cross sections as per Eq. (35); — — —, only direct cross sections according to Eq. (16).

channel is a moderate enhancement of the direct cross section. Note that in the $k\sigma$ channel the effective conjugate part vanishes and the only conjugate contributions are those included in the effective direct part.

The nonresonant $k\pi$ channels show a strikingly different behavior for the two satellites. For $S0$ we find a very small $k\pi$ cross section at threshold, followed by a steady increase to a shallow maximum 40 eV above, and a slow decline for higher energy. The conjugate contributions here lead to a substantial lowering of the direct $k\pi$ cross section, amounting to 40% at threshold. For $S1$, on the other hand, the conjugate contributions induce a drastic enhancement of the $k\pi$ cross section and lead to a steeply rising curve for decreasing photon energy. At threshold the entire $k\pi$ cross section is about five times larger than the direct value. Note that even at 100 eV above threshold the enhancement by the conjugate contributions still amounts to 30%. Obviously, the different impact of the conjugate contributions to the $S0$ and $S1k\pi$ cross sections is an effect of negative and positive interference, respectively, in the transition amplitude, where the different sign of the spectroscopic amplitudes $x_{1s}$ and the larger (by $\sqrt{3}$) effective conjugate part for $S1$ play an essential role.

To see the effect of interference more clearly we have plotted in Fig. 4 the "effective conjugate" cross section $\bar{\sigma}_0$ for $S0$ obtained by using in Eq. (34) the spin-free amplitude

$$\bar{I}_{lm\mu}=\tfrac{1}{2}\sqrt{2}\langle\bar{\Phi}_0^N|\Phi_0^N\rangle\langle\langle\psi_{\pi^*\bar{\mu}}|\hat{r}_\mu|\phi_{1s}\rangle\rangle\langle\langle\psi_{klm}^{(-)}|\phi_{\pi\bar{\mu}}\rangle\rangle\ , \tag{37}$$

where the effective direct part of the full amplitude (35) has been omitted. The corresponding quantity for $S1$ is simply $\bar{\sigma}_1=3\bar{\sigma}_0$. The effective conjugate cross sections $\bar{\sigma}_0$ and $\bar{\sigma}_1$ for the $\pi$-$\pi^*$ shakeup satellites are, to within constants, equal to the quantity $s_{1\pi}(k)$ that has been introduced in I [Eq. (95)] as a measure of the overlap between the $1\pi$ orbital and the $\pi$ continuum. As one would expect, the "squared overlap" $s_{1\pi}(k)$ is largest at threshold ($k\rightarrow 0$) and drops rapidly with increasing energy. The importance of interference effects for the magnitude of the cross sections is seen most strikingly at threshold where the full $k\pi$ cross section for $S1$ is three times as large as the effective conjugate cross section, and six times larger than the separate direct contribution.

How do the RCHF results agree with the experimental findings? Figure 5 shows the relative satellite intensities (branching ratios) as observed in recent synchrotron radiation studies [30]. Although to some extent these data may still reflect some experimental difficulties, there seems to be firm evidence for the major trends: the substantial increase of the $S1$ intensity, in contrast to the vanishing of the $S0$ satellite, for low photon energies. A near-threshold branching ratio of over 10% for $S1$ was deduced from these synchrotron studies. The $S0$ satellite, on the other hand, could only be traced down to about 350 eV, since for lower energy its intensity became too small and could no longer be separated from the background signal. Figure 5 also shows our calculated branching ratios. The C $1s$ single-hole cross section was

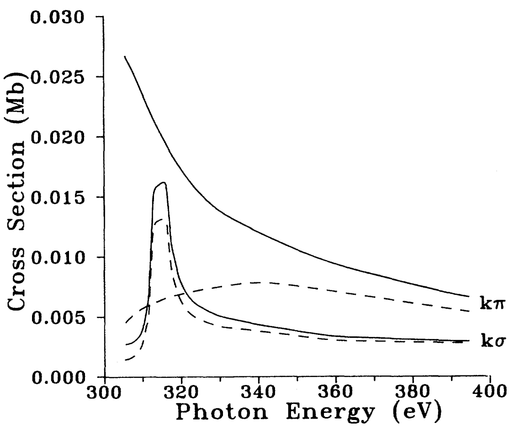

FIG. 3. Same as Fig. 2 for the $S1$ satellite of $CO^+$ (C $1s^{-1}$).

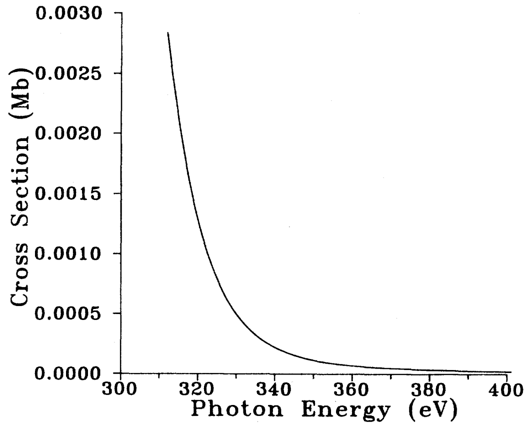

FIG. 4. Effective conjugate cross section $\bar{\sigma}$ of Eq. (37) for the $S0$ satellite.

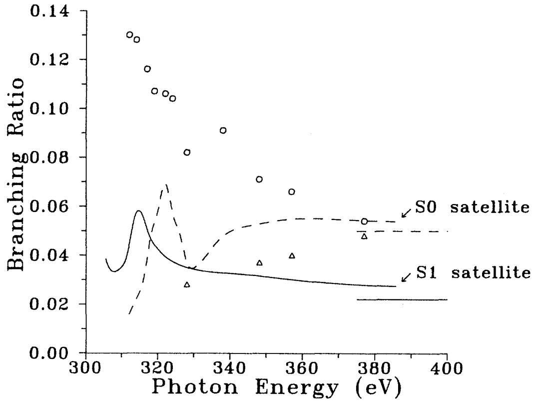

FIG. 5. Branching ratios (intensities relative to the C $1s^{-1}$ hole main peak) for the $S1$ and $S0$ satellites: —— and — — —, present results for $S1$ and $S0$, respectively; ——○—— and — — —△— — —, experimental results of Ref. [30] for $S1$ and $S0$, respectively. The horizontal lines show the high-energy (Al $K\alpha$) branching ratios for these satellites (Refs. [1] and [29]).

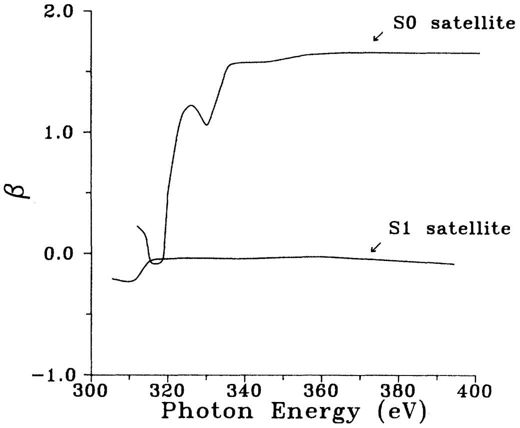

FIG. 6. Photoelectron asymmetry parameters for photoionization leading to the $S1$ and $S0$ satellites of $CO^+$ (C $1s^{-1}$), respectively.

taken from the RCHF calculation described in I, using, however, the spectroscopic factor $x_{1s}=0.68$ from the Green's function calculation [27] instead of the slightly larger RCHF value of 0.79. One should note that the $\sigma^*$ shape resonance in the theoretical C $1s$ single-hole channel, and hence the corresponding modulation of satellite branching ratios, is about 2–3 eV too high.

An obvious disagreement with experiment is the strong resonance enhancement in the RCHF cross section for $S0$, suggesting that the $S1$ resonance may also be spurious. The nonresonant background, on the other hand, seems to give a qualitatively correct description of the experimental intensities. The increase of the theoretical $S1$ branching ratio with decreasing energy is correctly predicted; though less pronounced than in the experimental curve, the theoretical near-threshold values are 6% or 4% with and without consideration of the $\sigma^*$ resonance, respectively. Disregarding the resonance in the $S0$ channel, extrapolation would predict a very small cross section and branching ratio at threshold. Towards higher energy the $S0$ curve rises to a maximum at 340 eV and approaches its asymptotic value slowly from above. The experimental $S0$ branching ratios lie somewhat below the theoretical curve and seem to yield the asymptotic value from below. While in some respects the picture drawn by the present calculation is quite satisfactory the question remains of how to explain the spurious resonance structures. The answer must be sought in specific shortcomings of the present theoretical treatment, such as the neglect of the target polarization induced by the continuum electron (in the $\sigma^*$ orbital) and the use of scattering potentials constructed from nonoptimized relaxed orbitals. Probably the $\sigma^*$ double-excitation resonances have to be expected at distinctly lower energies, possibly even below the respective thresholds.

Figure 6 shows the calculated photoelectron asymmetry parameters $\beta$. The resonance in the $S0$ channel is reflected in the $\beta$ curve by a sharp rise from a minimum ($\beta \simeq 0$) below the resonance position and a plateaulike behavior ($\beta \simeq 1.7$) above 340 eV. The $\beta$ curve shows a distinct dip centered at 330 eV, coinciding with the local minimum in the $S0$ cross section. The $\beta$ curve for $S1$ seems to be somewhat unusual: a small step around the calculated resonance is followed by a plateaulike shape with $\beta$ around 0.

Finally, we will briefly consider the monopole-forbidden satellite states associated with the configuration $(2\pi)^1(1s)^{-1}(1\pi)^{-1}$. According to the results of Ref. [27] there are four states in the order $^2\Delta$, $^2\Sigma^-$, $^2\Delta$, and $^2\Sigma^-$ at energies 9.7, 9.8, 11.1, and 11.4 eV, respectively, relative to the C $1s$ single-hole state. The energy separation between the states of the same symmetry is much smaller than for the pair of $^2\Sigma^+$ states and their characterization as triplet and singlet $\pi$-$\pi^*$ excitations is much less justified than in the latter case. Assuming the latter coupling scheme nevertheless, the cross sections for the states $^2\Sigma^-(0)$, $^2\Sigma^-(1)$, $^2\Delta(0)$, and $^2\Delta(1)$ are simply given by $\bar{\sigma}_0$, $3\bar{\sigma}_0$, $2\bar{\sigma}_0$, and $6\bar{\sigma}_0$, respectively, where $\bar{\sigma}_0$ is the effective conjugate cross section as specified for $S0$ in Eq. (37). Note that these expressions reflect the statistical ratios of the respective satellite multiplets. Apart from slight differences due to the specific target potentials, the $\bar{\sigma}$ curves for the monopole-forbidden satellites will be similar to the curve shown in Fig. 4. Since the $\bar{\sigma}_0$ value at threshold is an order of magnitude smaller than the $S1$ cross section and drops sharply toward higher energy it will be difficult to detect these examples of pure conjugate shakeup in the experimental spectrum.

## VI. SUMMARY AND CONCLUSIONS

The relaxed-core Hartree-Fock (RCHF) approximation has been used to calculate energy-dependent intensities of shakeup satellites in the $K$-shell photoionization of atoms and molecules. As an example we have considered the $\pi$-$\pi^*$ satellites in the C $1s$ photoelectron spectrum of CO. The formulation given in I for $N$-electron transition moments involving determinants with mutually nonorthogonal orbitals has been adapted to the treatment of *K*-shell shakeup satellites. As in I, use has been made of the core-valence separation (CVS) approximation which is justified here by the large energy difference and the small coupling matrix elements of states with different *K*-shell occupations. The CVS approximation leads to a considerable simplification of the RCHF transition moments and eliminates the problems of nonorthogonality between the initial and final *N*-electron state. As a further modification of the RCHF scheme, we have adjusted the static (energy-independent) spectroscopic amplitudes $x_{1s}^{(n)}$ to values obtained from large-scale *ab initio* calculations, thereby matching the relative satellite intensities to their theoretical (and experimental) branching ratios in the limit of high photon energy.

The essential finding of the present calculations for the pair $(S0,S1)$ of C 1*s* $\pi$-$\pi^*$ satellite states in CO are strong interference effects between the direct (bound-free dipole integral) and conjugate (bound-free overlap integral) contributions in the transition moment at near-threshold energies. These effects are particularly dominant in the $k\pi$ subchannel and, for the triplet-coupled satellite $S1$, lead to a drastically increasing cross section with decreasing photon energy. For the singlet-coupled satellite $S0$, on the other hand, we find destructive interference resulting in comparatively small values of the cross section near threshold.

These interference effects seem to provide an explanation for the strikingly different behavior of the experimentally observed satellite intensities. It should, however, be recalled that the near-threshold enhancement of the $S1$ branching ratio, deduced from the experiments of Ungier and Thomas [9] and of Reimer *et al.* [8], is even more pronounced than in the present description. Ungier and Thomas [9] have rationalized the enhanced $S1$ cross section as an effect of conjugate shakeup. The role of the different target potentials for $S0$ and $S1$, which is discussed by Reimer *et al.* [8] as a possible reason for the different satellite intensities near threshold, seem to be of minor relevance [9]. The importance of direct-conjugate interference is underlined by the fact that pure conjugate shakeup, observable, e.g., in the monopole-forbidden $\pi$-$\pi^*$ satellites, is not effective except perhaps at energies very close to threshold.

In both satellite channels the RCHF results show distinct $\sigma$ shape resonances about 10 eV above threshold. The position and even the occurrence of these resonances are questionable, and they may well be artifacts of our calculation. At least for $S0$, the experimental results clearly discard any resonance enhancement down to 2–3 eV above threshold. This apparent discrepancy suggests possible shortcomings of the present theoretical treatment. We have already mentioned that the RCHF representation of the target states could possibly be improved by state-specific relaxed orbitals. Also the neglect of double excitations, which are substantially admixed in the optimized $S0$ satellite state, may play a role. A more severe shortcoming also becomes apparent in our perturbation-theoretical analysis of the RCHF transition moment: already in first-order dynamically important contributions are missing, namely a correlation contribution arising from initial-state correlations and a polarization contribution due to the response of the target to the photoelectron. Thus the RCHF description of shakeup satellites is inferior to that of the single-hole main state where the RCHF transition moment is complete through first order (in the CVS approximation). One must be aware that upon inclusion of these energy-dependent contributions the picture given here may yet change considerably.

## ACKNOWLEDGMENTS

J.S. acknowledges funding by the Federal Ministry for Research and Technology (Germany) under Contract No. 05 352AX-3. This work was also supported by the National Science Foundation through Grant No. CHE-8521391.

---

*Present address: T-12 Division, Mail Stop B-268, Los Alamos National Laboratory, Los Alamos, NM 87545.

[1] U. Gelius, J. Electron Spectrosc. Relat. Phenom. **5**, 985 (1974).
[2] H. Siegbahn and L. Karlsson, in *Handbuch der Physik*, edited by W. Mehlhorn (Springer, Berlin, 1982), Vol. 31.
[3] T. A. Carlson and M. O. Krause, Phys. Rev. **140**, A1057 (1965).
[4] T. Åberg, Phys. Rev. **156**, 35 (1967).
[5] P. H. Kobrin, S. Southworth, C. M. Truesdale, D. W. Lindle, U. Becker, and D. A. Shirley, Phys. Rev. A **29**, 194 (1984).
[6] C. M. Truesdale, D. W. Lindle, P. H. Kobrin, U. E. Becker, H. G. Kerkhoff, P. A. Heimann, T. A. Ferret, and D. A. Shirley, J. Chem. Phys. **80**, 2319 (1984).
[7] D. W. Lindle, C. M. Truesdale, P. H. Kobrin, T. A. Ferret, P. A. Heimann, U. Becker, H. G. Kerkhoff, and D. A. Shirley, J. Chem. Phys. **81**, 5375 (1984).
[8] A. Reimer, J. Schirmer, J. Feldhaus, A. M. Bradshaw, U. Becker, H. G. Kerkhoff, B. Langer, D. Szostak, R. Wehlitz, and W. Braun, Phys. Rev. Lett. **57**, 1707 (1986); J. Phys. (Paris) Colloq., Suppl. 12 **48**, C9-773 (1987).
[9] L. Ungier and T. D. Thomas, Phys. Rev. Lett. **53**, 435 (1984).
[10] L. J. Medhurst, T. A. Ferret, P. A. Heimann, D. W. Lindle, S. H. Liu, and D. A. Shirley, J. Chem. Phys. **89**, 6096 (1988).
[11] Ishihara, J. Mizuno, and T. Watanabe, Phys. Rev. A **22**, 1552 (1980).
[12] W. Wijesundera and H. P. Kelly, Phys. Rev. A **39**, 634 (1989).
[13] H. Ågren and V. Carravetta, J. Chem. Phys. **87**, 370 (1987).
[14] J. W. Gadzuk and M. Šunjić, Phys. Rev. B **12**, 524 (1975).
[15] H. W. Meldner and J. D. Perez, Phys. Rev. A **4**, 1388 (1971).

[16] T. D. Thomas, Phys. Rev. Lett. **52**, 417 (1984).

[17] V. McKoy, T. A. Carlson, and R. R. Lucchese, J. Phys. Chem. **88**, 3188 (1984).

[18] J. Schirmer, M. Braunstein, and V. McKoy, Phys. Rev. A **41**, 283 (1990).

[19] J. Berkowitz, J. L. Dehmer, Y. -K. Kim, and J. P. Desclaux, J. Chem. Phys. **61**, 2556 (1974).

[20] R. L. Martin and D. A. Shirley, J. Chem. Phys. **64**, 3685 (1976).

[21] A. Arneberg, J. Müller, and J. Manne, Chem. Phys. **64**, 249 (1982).

[22] I. Cacelli, V. Carravetta, and R. Moccia, J. Phys. B **16**, 1985 (1983).

[23] J. Schirmer, G. Angonoa, and L. S. Cederbaum, Z. Phys. D **5**, 253 (1987).

[24] For example, see B. H. Bransden, *Atomic Collision Theory* (Benjamin, New York, 1970).

[25] R. R. Lucchese and V. McKoy, Phys. Rev. A **21**, 112 (1980).

[26] R. R. Lucchese, K. Takatsuka, and V. McKoy, Phys. Rep. **131**, 147 (1986).

[27] G. Angonoa, O. Walter, and J. Schirmer, J. Chem. Phys. **87**, 6789 (1987).

[28] J. Schirmer, G. Angonoa, S. Svensson, D. Nordfors, and U. Gelius, J. Phys. B **20**, 6031 (1987).

[29] M. F. Guest, W. R. Rodwell, T. Darko, I. H. Hillier, and J. Kendrick, J. Chem. Phys. **66**, 5447 (1977).

[30] J. Feldhaus and A. M. Bradshaw (private communication).